Revue des Composites et des Matériaux Avancés-Journal of Composite and Advanced Materials
Vol. 36, No. 3, June, 2026, pp. 623-635
Journal homepage: http://iieta.org/journals/rcma

Quercetin-Loaded Polycaprolactone Electrospun Mats as Bioactive Wound Dressings: Fabrication, Characterization, and in Vivo Evaluation

Asmaa A. Oleiwi*, Ghaidaa S. Hameed

Department of Pharmaceutics, College of Pharmacy, Mustansiriyah University, Baghdad 10052, Iraq

Corresponding Author Email: asmaaassim95@uomustansiriyah.edu.iq

https://doi.org/10.18280/rcma.360316

Received: 12 February 2026
Revised: 24 April 2026
Accepted: 4 May 2026
Available online: 30 June 2026

Keywords:
electrospinning technology, nanofibrous membranes, drug-loaded fibers, wound healing, postsurgical dressing

ABSTRACT

Electrospun nanofibrous wound-dressing materials have been identified as potential carriers for therapeutic drug delivery and enhanced wound healing processes, creating a favorable environment for the healing process. In this study, quercetin-loaded polycaprolactone (PCL) nanofibrous mats with different concentrations of quercetin (1, 3, 5, and 10 wt.%) were produced using the electrospinning method. Field emission scanning electron microscopy (FE-SEM), X-ray diffraction (XRD), and differential scanning calorimetry (DSC) analyses were conducted for characterization of the morphology, crystallinity, and thermal behavior of the nanofibrous membranes formed. Based on the results, quercetin was effectively immobilized onto the surface of PCL nanofibers primarily in an amorphous state. Nevertheless, a higher concentration of quercetin led to increased diameters of the fibers and decreased morphological uniformity. High efficiency of drug entrapment was attained, but its value tended to decrease with the increase in the quercetin concentration due to possible saturation of the polymer matrix and agglomeration of quercetin molecules. Among the samples produced, the electrospun mat loaded with 5 wt.% quercetin demonstrated the highest efficiency of encapsulation (93%), contact angle (109.9°), and cumulative release of quercetin molecules (56.9%, 70.5%, and 81.6% within 24, 72, and 168 hours, respectively). According to in vivo histological studies, there was a significant enhancement in the group treated with the PCL loaded with 5% quercetin (Q) nanocomposite material, evidenced by the absence of inflammation, increased collagen deposition, and accelerated re-epithelialization at day 21 ($p < 0.05$). Thus, electrospun mats loaded with 5 wt.% quercetin may be viewed as a prospective bioactive wound dressing.

1. INTRODUCTION

Wound healing can be defined as a multifaceted biological process that entails repairing injured tissues by passing through several stages, such as hemostasis, inflammation, proliferation, and remodeling [1]. Poor wound management can elevate healthcare expenses, facilitate chronic wound formation, and delay healing processes, underscoring the necessity of proper wound dressings [2].

Wound dressings are usually classified as traditional or advanced dressings depending on their characteristics. Traditional wound dressings have mostly been passive and non-occlusive with minimal interaction with the wound site. These materials lack moisture-retention abilities, manage minimal amounts of exudate, and cause discomfort during dressing removal [1, 3]. To overcome these limitations, current wound care practices have focused on bioactive dressings, with electrospinning-based nanofibrous dressings attracting considerable interest [4]. Electrospinning technology allows the fabrication of three-dimensional structures with diameters of sub-micron to nanometer scale, providing a substantial amount of surface area and porosity to imitate the natural extracellular matrix and create a favorable environment for healing [5].

Electrospinning is a very sensitive process that depends on many solution, process, and environmental factors. Such factors provide control over fiber morphology, porosity, and loading capacity, which are key parameters for wound healing dressings [6]. As for synthetic materials, polycaprolactone (PCL) is frequently applied for the development of wound dressings due to its biological and mechanical properties. However, the fact that PCL is hydrophobic and semi-crystalline is an explanation for its slower degradation process. But electrospun PCL degrades faster due to a high surface area-to-volume ratio [7]. In addition, to improve the biological activity of PCL-based scaffolds, quercetin, a naturally occurring flavonoid, has been incorporated into the system. Quercetin has well-known antioxidant and anti-inflammatory properties, which may be beneficial in the wound healing process. However, its clinical application is limited by its poor solubility in water [8, 9].

One effective method to minimize this limitation is to

disperse quercetin in amorphous forms of the matrix. Electrospinning is a key process in the drug amorphization mechanism because it favors the quick solvent-solidification process in the drug-polymer solution. Thus, the formation of crystallinity in the quercetin compound is avoided [10, 11].

While quercetin's biological properties and electrospun nanofibrous membranes have been extensively studied for wound healing applications, a few studies have investigated quercetin-loaded PCL mats as a material for surgical incision wound healing [12, 13]. Most studies have focused on quercetin-loaded topical formulations, hydrogels, or general wound dressing membranes. However, the effects of quercetin loading concentration on the overall performance of PCL electrospun mats have not been sufficiently clarified. In this study, quercetin-loaded PCL electrospun mats were designed and characterized to determine the influence of different quercetin concentrations on the structural, surface, pharmaceutical, and biological properties of the nanofibers. PCL was selected as a biocompatible and biodegradable polymeric scaffold for the formation of fibers owing to its ability to provide mechanical strength, structural stability, and controlled quercetin release. Quercetin was added as a bioactive compound due to its antioxidant and anti-inflammatory capabilities that may contribute to collagen deposition, re-epithelialization, and tissue regeneration. The selected solvent system and polymer concentration were used to get the required spinnable solution to produce continuous nanofibers with acceptable structural properties. A linear incision model was adopted since it mimics the closed wounds that occur following surgery, where the mat will have to provide support and localized drug delivery at the site of injury.

As shown in Table 1, previous studies have explored quercetin-loaded electrospun systems that primarily focused on PCL-based systems, composite polymers, nanoparticles embedded in scaffolds, or more widely loaded polyester fibers with antioxidant molecules. However, these studies have revealed some improvements in wettability, antibacterial effects, biocompatibility, sustained drug delivery ability, and wound healing capacity. However, most previous studies introduced additional materials like graphene oxide, gelatin, or copper oxide nanoparticles, making it difficult to isolate the specific effect of quercetin in the PCL system. Moreover, histological evidence supporting wound healing remains limited. Therefore, further investigation is needed to clarify how quercetin concentration affects the structure, wettability, and drug-release behavior of electrospun PCL mats.

Table 1. Summary for polycaprolactone (PCL)/quercetin-based electrospun system studies

Ref.	Formula	Application	Main Results	Gap / Relevance to the Present Study
[14]	Quercetin-mediated CuO nanoparticles incorporated into PCL electrospun scaffold	Antibiofilm and antibacterial wound-related scaffold	The scaffold targeted Pseudomonas aeruginosa biofilm and showed wound-related antibacterial potential.	The effect was mainly related to quercetin-mediated CuO nanoparticles; therefore, the independent effect of quercetin loading concentration in PCL mats was not clarified.
[13]	PCL/graphene oxide/quercetin electrospun scaffold	Wound dressing and tissue engineering	The scaffold was evaluated for structural, antibacterial, and cell-related properties.	The presence of graphene oxide makes it difficult to isolate the direct effect of quercetin concentration on PCL electrospun mats.
[15]	PCL/gelatin/quercetin electrospun nanofibers	Wound dressing application	The nanofibers showed favorable morphology, improved hydrophilicity, sustained release, antibacterial activity, fibroblast compatibility, and enhanced wound healing.	The study used a PCL/gelatin hybrid system; therefore, the effect of quercetin loading concentration in PCL-only mats remains insufficiently explained.
[16]	Polyester electrospun fibers containing antioxidants, including quercetin	Antioxidant-loaded electrospun system for tissue repair-related applications	The study investigated antioxidant-loaded polyester fibers and included quercetin as one of the antioxidant compounds.	The study was broader and compared different antioxidants; it did not focus specifically on quercetin-loaded PCL mats or surgical wound healing.
Present study	PCL electrospun mats loaded with different quercetin concentrations	Optimization of quercetin-loaded PCL mats for wound-healing application	The present study evaluates the quercetin concentration effect on morphology, wettability, encapsulation efficiency, release profile, and in vivo wound healing activity.	This study addresses the gap by focusing on concentration-dependent quercetin loading in PCL electrospun mats without additional nanoparticles or secondary bioactive agents.

This study aimed at a systematic assessment of the dose-dependent effects of quercetin incorporation into electrospun PCL mats. Specifically, the impact of drug incorporation on the morphology, wettability, loading efficiency, release profile, kinetics, and biological performance of PCL electrospun mats in a surgical incision wound model was assessed. Furthermore, histological examination was carried out for the assessment of wound healing at the tissue level.

2. EXPERIMENT PART

2.1 Materials

PCL (Mw 250,000 gm/mol) was the primary polymeric carrier and was provided by American Polymer Services, Inc. (APS, USA). Quercetin (≥95% purity) was sourced from Sigma-Aldrich (St. Louis, MO, USA). The solubilizer used in the release media, Tween 80, was provided by Central Drug

House Ltd. (India). Ethanol (analytical grade, ≥99.9%) and glacial acetic acid (analytical grade, ~99%) were both provided by Sigma-Aldrich and CARLO ERBA Reagents (Italy), respectively.

2.2 Mats preparation

The electrospinning method was employed to create PCL nanofibrous membranes. The PCL was dissolved in glacial acetic acid (~99%) using magnetic stirring at 500 rpm for 4 hours at ambient temperature to get 12 wt.% homogeneous solution. Subsequently, quercetin was added to the mixture at different concentrations of 1, 3, 5, and 10 wt.% based on PCL weight, whereas Tween 80 was introduced at 0.8 wt.% as a surfactant. The resulting mixture was stirred overnight, and probe sonication for 3 min was performed using an ultrasonic homogenizer (Model 300VT, USA) to eliminate any aggregates and bubbles.

The prepared solutions were electrospun with the aid of a bio-electrospinning/electrospray system (ESB-200, South Korea). In this respect, each solution was placed in a 10 mL syringe and dispensed via a stainless steel 23-gauge needle at a constant flow rate of 1 mL/h. The voltage and distance between the needle and the collector plate were set to 20 kV and 18 cm, respectively. The electrospinning process was carried out for 2 hours under ambient conditions of 25 ± 2 ℃ and 40 ± 5% relative humidity, as depicted in Figure 1.

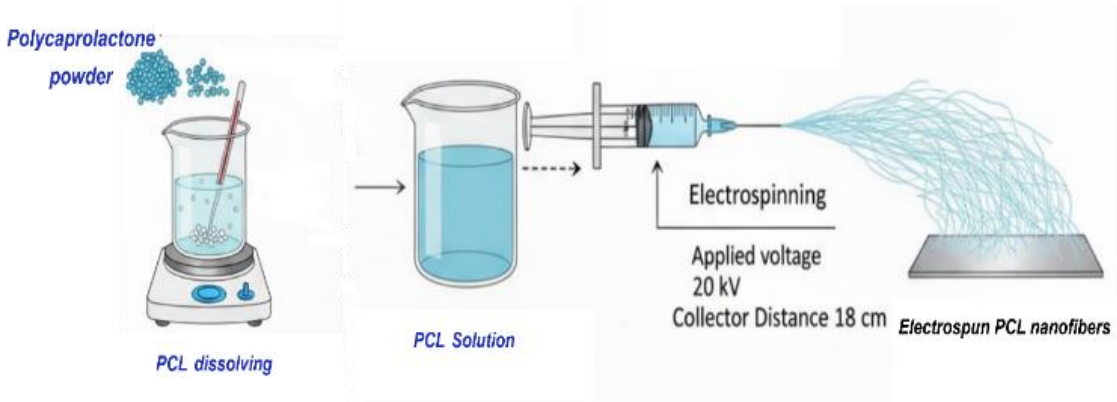

Figure 1. Electrospinning of polycaprolactone (PCL) mat steps

2.3 Characterization

Properties of the electrospun mats were characterized in order to study their morphology, structure, thermal properties, chemical nature, and function, as well as drug encapsulation and release.

2.3.1 Properties of electrospinning solution

Viscosity of electrospinning solutions was determined at room temperature using a Brookfield viscometer (DV-II PRO, USA) with spindle No. 4 at 100 rpm. Measurements were carried out after stabilization and repeated three times.

Electrical conductivity of solutions was determined at room temperature using a conductivity meter (Cond 7110). Before the experiment, the device was calibrated, and measurements were carried out after stabilization. Conductivity was measured three times for each solution and expressed as the mean ± SD.

2.3.2 Weight variation and thickness of the electrospun mats

Weight variation was studied by taking squares from each formulation, measuring 2 cm × 2 cm in size. Three pieces were randomly selected from each formulation and weighed using an analytical balance. Thickness was determined by digital Vernier calipers at five different positions, including a central one and four peripheral ones.

2.3.3 Morphological characterization

Morphology of the electrospun scaffolds was analyzed using the field emission scanning electron microscopy (FE-SEM) technique (Zeiss, Germany). The SEM images were used for evaluation of the fiber uniformity, surface morphology, presence of beads, fiber diameter, pore size, and porosity. Fiber diameter and pore size were quantitatively determined using ImageJ software by taking at least 100 measurements.

2.3.4 Wettability test

The wettability of the electrospun membranes was determined using water contact angle measurements on a contact angle analyzer (CAM 110, Germany). A drop of distilled water was applied to the membrane surface, and the angle was measured after about 3 seconds using the instrument's image-analysis software.

2.3.5 Crystalline structure analysis

The crystalline structure of the synthesized membranes was studied using X-ray diffraction (XRD) analysis performed on a Philips PW1730 diffractometer (Netherlands). The measurements were carried out using Cu Kα radiation (λ = 1.5406 Å) at 40 kV and 40 mA over a 2θ range of 3°–32°. The obtained diffraction curves were used for comparison to investigate the crystal form of PCL and the effect of quercetin addition.

2.3.6 Thermal analysis

Thermal behavior of the samples was studied using differential scanning calorimetry (DSC). For that purpose, approximately 5 mg of each sample was sealed in an aluminum pan and subjected to heating from 20 ℃ to 500 ℃ at a rate of 10 ℃/min in a nitrogen atmosphere (flow 60 mL/min).

2.3.7 Fourier transform infrared spectroscopy

Fourier transform infrared spectroscopy (FTIR) was conducted with a Bruker Tensor 27 FTIR spectrometer

(Germany), which was used to characterize the functional groups and potential interactions between PCL and quercetin. Changes in the position or intensity of the peaks were analyzed to compare the spectra of both pure samples and quercetin-loaded PCL scaffolds.

2.3.8 Saturated solubility test

The saturated solubility of quercetin was evaluated by dissolving an excess amount of quercetin in a 20 mL solution of phosphate buffer (0.8% Tween 80, pH 7.4) under stirring conditions at 400 rpm and room temperature (25 ℃) for 72 h. Afterwards, the filtrate was quantitatively determined for the concentration of quercetin with a UV-Vis spectrophotometer at the maximum absorption wavelength of the drug.

2.3.9 Calibration curves

The calibration curves of quercetin release were carried out in PBS buffer (pH 7.4) with 0.8% Tween 80. In the case of the encapsulation efficiency experiment, the calibration curve was developed in ethanol with 5% v/v glacial acetic acid, which is the same solvent as that for the extraction of the nanofibers. The solvent used in the extraction of the nanofibers is the same as mentioned above. Stock solutions were prepared at concentrations of 15 µg/mL in PBS medium and 13 µg/mL in ethanol with 5% v/v glacial acetic acid. Various dilutions were performed in order to prepare different concentrations of quercetin solutions from the stock solution. The dilution was done at concentrations of 1.5, 3, 4.5, 6, 7.5, 9, 10.5, 12, and 13.5 µg/mL in PBS pH 7.4 and 1.3, 2.6, 3.9, 5.2, 6.5, 7.8, 9.1, 10.4, and 11.7 µg/mL in ethanol. The absorbances were determined using a UV-Visible Spectrophotometer Shimadzu (Japan) at wavelengths 373 nm and 376 nm for ethanol and PBS media, respectively.

2.3.10 Encapsulation efficiency determination

The quantitative determination of the encapsulation efficiency of quercetin entrapment by electrospun nanofibers was done by dissolving 10 mg of the electrospun samples with 0.5 mL of glacial acetic acid. Ethanol was then added gradually while stirring the solution until reaching a total volume of 10 mL, thereby obtaining an extraction solution of 5% v/v glacial acetic acid in ethanol. The solution was then centrifuged at 2000 rpm for 15 minutes in order to eliminate polymer residues. Prior to UV-Vis spectroscopy of the solution, the sample was filtered to eliminate interference caused by the polymer. The absorbance was measured using a UV-Vis spectrophotometer at $\lambda = 373$ nm.

Quercetin content was determined based on the calibration curve of quercetin in ethanol with 5% v/v glacial acetic acid, since it is the solvent used for nanofiber extraction. Solvent blanks were used for baseline adjustment. All measurements were carried out in triplicate, and all values reported are means ± standard deviation (SD). The encapsulation efficiency (EE) is given by Eq. (1):

$$EE = \frac{amount\ of\ quercetin\ in\ mat}{theoretical\ of\ quercetin\ in\ mat} \quad (1)$$

2.3.11 In vitro drug release study

The procedure for in vitro release was as follows: the electrospun mat with an average weight of about 18 mg was suspended in 25 mL of a PBS (pH 7.4) solution containing 0.8% Tween 80. The test was performed at 37 ℃, with magnetic stirring at 50 rpm. All release containers were protected by aluminum foil from quercetin photolysis. At specific time points (1, 2, 3, 6, 12, 24, 48, 72, 96, 132, 168, 200, 240, 270, 300, and 330 h), 2 mL of the release solution was collected, filtered with a 0.45 µm syringe filter, and quantified by spectrophotometry at 376 nm. The removed aliquots were replaced immediately with an equivalent volume of fresh release medium [17]. The release percentage was cumulatively calculated from the amount of quercetin that had been released from the sample, as determined from the encapsulation efficiency test using the calibration graph generated earlier. This was done in triplicate (n = 3).

2.3.12 Statistical analysis

All tests were carried out in triplicate, and the data were presented as mean ± SD. Analysis of variance (ANOVA) was used for comparing the values of encapsulation efficiency and viscosity, with $p < 0.05$ being taken as statistically significant. In terms of the histological study, the semi-quantitative score of hematoxylin and eosin (H&E)-stained sections was subjected to two-way ANOVA with Tukey's post hoc test to find out the effect of treatment and healing period on the outcomes.

2.4 In vivo wound healing evaluation

In total, 27 adult male Wistar rats, each weighing 250 ± 20 g, were employed in the in vivo study. The animals were housed individually in wire cages at the laboratory with unlimited access to standard pelleted food and water in order to get acquainted with their new surroundings. After the acclimatization phase of 15 days, the animals were randomized into the following groups.

The animals were randomly assigned to experimental groups at random prior to wound induction. Histopathological assessment was conducted in a blinded manner, whereby the evaluator was not aware of the group to which the animal belonged when assigning scores. The exclusion criteria were predefined and included significant wound infection, wound dehiscence, postoperative mortality not attributed to treatment and poor quality of histopathological slides. Postoperatively, the animals were evaluated daily for their overall health, wound healing, eating habits, and signs of pain.

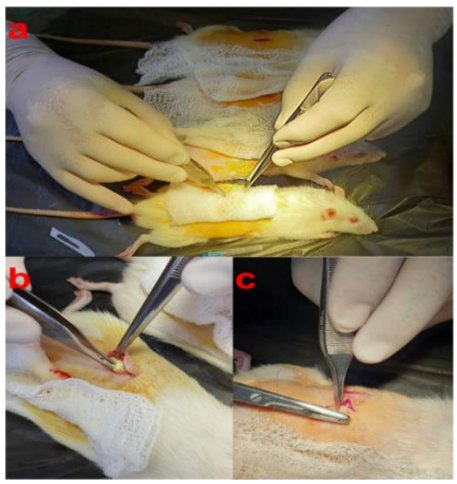

Figure 2. The in vivo surgical process involved the implantation of the electrospun mat. (a) Preparation of the dorsal surgical site and formation of a full-thickness wound, (b) application of the polycaprolactone (PCL) or quercetin-loaded PCL electrospun mat to the wound site, and (c) closure of the wound with sutures

A standardized full-thickness linear incision wound of about 4 cm long was surgically induced on the back of the animal. As shown in Figure 2, the standardized wound model was induced. Animals in Group A are seen as the untreated controls. Similarly, Group B received pure PCL mats. Group C received quercetin-loaded PCL mats.

Before surgery, the animals were fasted for 2 h and anesthetized by intraperitoneal administration of ketamine hydrochloride (75 mg/kg) combined with xylazine hydrochloride (10 mg/kg). The dorsal area was shaved along an approximately 8 cm midline region, followed by sequential disinfection of the operative site with chlorhexidine gluconate, 70% isopropyl alcohol, and 1.5% iodine tincture. All surgical procedures were performed aseptically while the animals were maintained in a ventral recumbent position.

In histopathology assessment, skin specimens were obtained from three animals per group at 7, 14, and 21 days post-surgery. The removed tissues were promptly placed in formalin, processed through standard histological techniques, embedded in paraffin wax, sectioned at 5 μm, and stained with H&E. The stained slides were analyzed under light microscopy to evaluate the degree of inflammatory cell accumulation, collagen deposition, epithelialization, and wound healing status.

All animal experiments were performed in accordance with the guidelines for the care and use of laboratory animals and were approved by the Institutional Animal Ethics Committee of the College of Pharmacy, Mustansiriyah University, Iraq (Approval No. 57). Appropriate measures were taken to minimize animal suffering and to reduce the number of animals used while maintaining reliable experimental outcomes.

3. RESULTS AND DISCUSSION

3.1 Measurement of viscosity and electrical conductivity for electrospinning solutions

The viscosity and conductivity of the electrospinning solutions are provided in Table 2. The results show that the viscosity levels increased gradually with an increase in the amount of quercetin used in each sample. This increase in viscosity levels was statistically significant for all samples ($p < 0.05$). However, in terms of electrical conductivity, only a slight increase in conductivity level was observed as quercetin content increased. It is apparent that both the quercetin concentration and polymer formulation played a role in defining the properties of electrospinning solutions and the mat.

3.2 Weight variation and thickness of electrospun mats

Weight variations and thickness of the prepared electrospun mats are presented in Table 3. The results signified that the weight of the mats was significantly associated with increased quercetin concentration in all formulations ($p < 0.05$). The mats also showed desirable weight uniformity within each formulation, as reflected by the relatively low SD values. Generally, the findings revealed that both the quercetin concentration and polymer formulation influenced the characteristics of the electrospun solutions and fabricated mats.

Table 2. Viscosity and electrical conductivity for electrospinning solutions (mean ± SD, n = 3)

Quercetin (wt.%)	Viscosity (cP)	Conductivity (mS/cm)
0	268 ± 2	0.1 ± 0.01
1	276 ± 3	0.2 ± 0.01
3	292 ± 4	0.2 ± 0.01
5	308 ± 3	0.2 ± 0.02
10	334 ± 5	0.3 ± 0.02

Table 3. Weight variations and thickness of the prepared electrospun mats (mean ± SD, n = 3)

Quercetin (wt.%)	Weight (mg)	Thickness (mm)
0	12 ± 1	0.16 ± 0.02
1	16.4 ± 2	0.17 ± 0.02
3	25 ± 2	0.18 ± 0.02
5	32 ± 1	0.2 ± 0.03
10	50 ± 3	0.23 ± 0.03

3.3 Morphological characteristics of polycaprolactone mats

The electrospun PCL nanofibers morphology is shown in Figure 3 and presents a uniform morphology of the electrospun PCL nanofibers. As can be seen from the figure, the pure PCL mat was uniformly structured without any bead formation, showing the formation of a stable electrospun jet. This shows the spinnability of the PCL solution, which resulted in a stable nanofibrous mat structure. It is clear from the figure that the electrospun mat consists of fibers having an average diameter of 129.6 ± 2.8 nm. The electrospun PCL fibers were selected as the base matrix to incorporate the drug due to their high surface area, fine fiber diameter, and porosity.

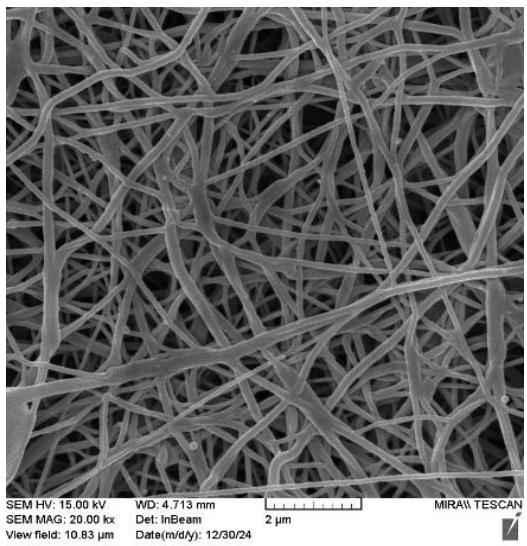

Figure 3. Field emission scanning electron microscopy (FE-SEM) image of the electrospun polycaprolactone (PCL) mat

Figure 4 presents the electrospun nanofibers morphology of PCL loaded with quercetin. As can be seen, the average diameter of the PCL nanofiber mat was determined to be 129.6 ± 2.8 nm. With the addition of quercetin, there was an observed increase in fiber diameter with concentration. At lower concentrations (1% and 3%), the fibers had smooth morphology with consistent size. However, with the increase in the concentration of quercetin to 5% and 10%, the fibers were found to be larger with rough morphology. The size of

the fiber increased to 165.4 nm for 5% quercetin loading, and for 10% quercetin loading, it was found to be 193.6 ± 5 nm. It is noteworthy that the electrospun fibers had no beads for the entire range of concentration studied [10, 18].

The increase in fiber diameter with increasing drug concentration may be attributed to changes in the physicochemical properties of the electrospun solution. In fact, a higher content of quercetin increased the viscosity of the solution and reduced its electrical conductivity, leading to a decrease in stretching forces acting on the jet of the electrospun solution [19]. Therefore, a reduced elongation of the jet results in fibers with larger diameters. Beyond a critical concentration, the quercetin molecules had the tendency to partially segregate and precipitate on the surface rather than being completely encapsulated in the polymer matrix; this induced a certain number of surface irregularities and a partial loss of structural homogeneity, as assessed from FE-SEM images.

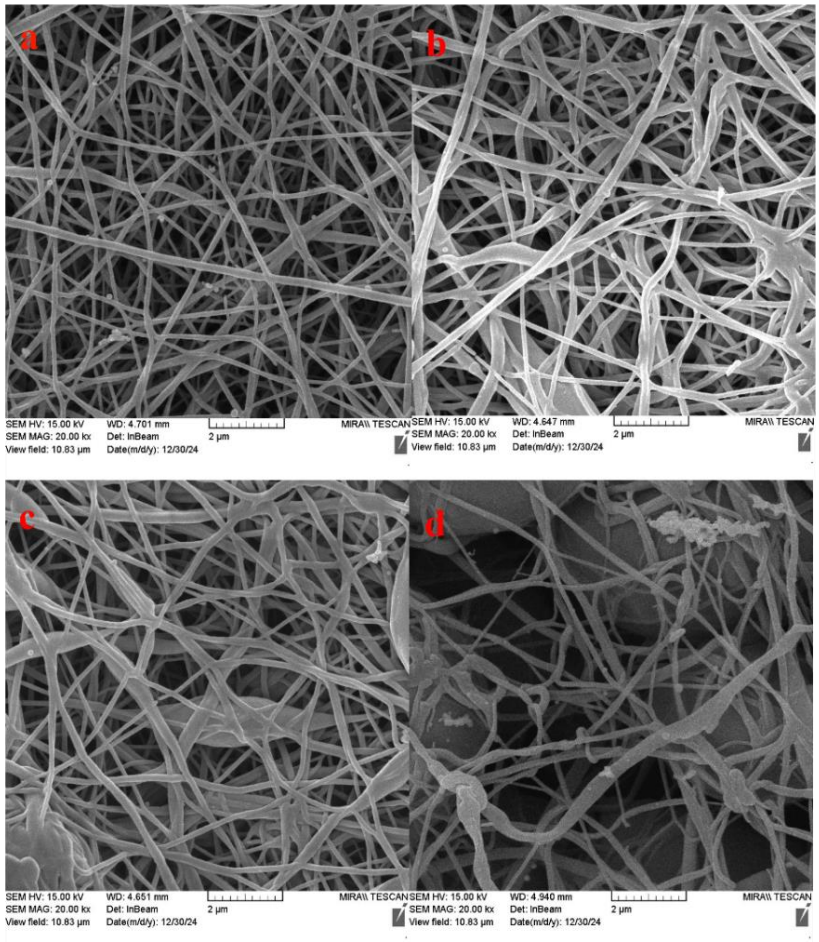

Figure 4. Field emission scanning electron microscopy (FE-SEM) images of quercetin-loaded polycaprolactone (PCL) mats by various concentrations, including (a) 1 wt.%, (b) 3 wt.%, (c) 5 wt.%, and (d) 10 wt.%

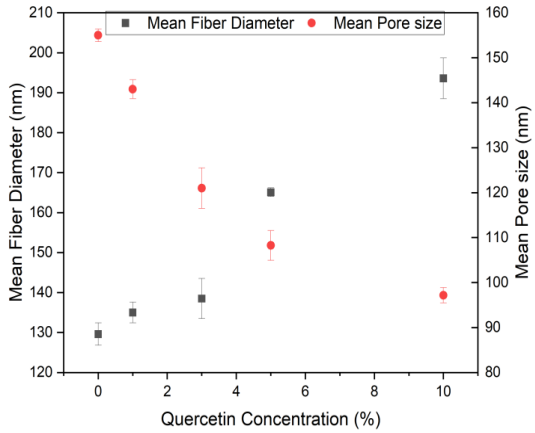

Figure 5. Average fiber diameter and pore size of polycaprolactone (PCL) mats in the presence of various quercetin concentrations

Note: Data are presented as mean ± SD of three SEM micrographs for each sample; at least 100 fibers and pores were analyzed using ImageJ software.

Figure 5 shows the dependence of the average fiber diameter and average pore size of electrospun mats on the quercetin concentration. The average pore size decreased with increasing concentration. This effect can be explained by the increased fiber diameter and closer fiber packing in the membrane structure. Pore properties play a significant role in the development of wound dressings because they affect cell migration, liquid permeability, gas exchange, drug release, and bacteria penetration [20]. It is important to control the porosity because it determines gas, nutrient, and exudate transportation; bioactive substance transport; and cellular attachment to the wound area. According to previous studies, the appropriate porosity in wound dressing scaffolds was between 60% and 90% [21, 22]. Porosity was calculated using the ImageJ program from FE-SEM images, and all obtained mats have the required porosity value.

3.4 Wettability

Figure 6 shows the influence of the concentration of

quercetin on the wettability of electrospun PCL membranes, as demonstrated by the water contact angles. The control sample showed the highest contact angle due to the inherent hydrophobic nature of PCL. As the drug concentration increased, there was a significant decrease in the contact angle. At 10% loading of quercetin, the contact angle reached its lowest point, around 92.4°. This indicates an improvement in the surface hydrophilicity of the electrospun membranes after incorporation of quercetin. The small decrease in the contact angle observed at lower concentrations could be attributed to the trapping of quercetin in the fibrous network of the membrane, thereby reducing its availability on the surface. However, at high concentrations, particularly 10%, the marked drop in the contact angle could be due to the enhanced availability of quercetin and its polar phenolic hydroxyl groups [15]. Localized moist microenvironment maintenance by the electrospun mat favored the softening and enzymatic degradation of the necrotic tissue [23]. Enhanced surface hydrophilicity may promote a moist wound environment, which is conducive to cell invasion, collagen deposition, and re-epithelialization.

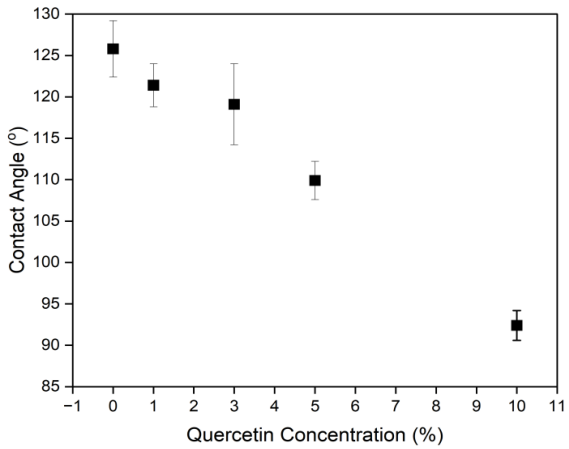

Figure 6. Illustration of the contact angle for polycaprolactone (PCL) mats in the presence of various quercetin concentrations
Note: Data are expressed as mean ± SD (n = 3).

3.5 X-ray diffraction

The XRD profiles for pure quercetin, the blank PCL electrospun mat, and quercetin-loaded PCL mats are illustrated in Figure 7. XRD technique was used to study the crystallinity of each component separately and to identify any structural variations that might occur following quercetin loading into the PCL nanofiber matrix. XRD profile of pure quercetin exhibited several sharp peaks at angles of approximately 11°, 13°, 14°, and 28°, thus demonstrating its crystallinity [24]. On the other hand, the pure PCL mat possessed the characteristic semi-crystalline structure of PCL, which consists of two major peaks at about 22° and 24°, indicating the (110) and (200) planes of the orthorhombic crystals of PCL. When quercetin was incorporated into the PCL nanofibers, their XRD patterns showed mainly the characteristic peak of PCL, while the distinctive crystalline Bragg diffraction peaks of quercetin were not clearly detected in the composite nanofibers [25]. The absence of these peaks may suggest a reduction in the crystalline nature of quercetin and its transformation toward a more amorphous state within the nanofibrous matrix. In addition, the intensity of PCL peaks decreased with increasing quercetin concentration [26]. The presence of quercetin may have partially interfered with the crystalline arrangement of PCL chains; nevertheless, additional investigation on crystallinity is needed for confirmation of the observation [12, 27].

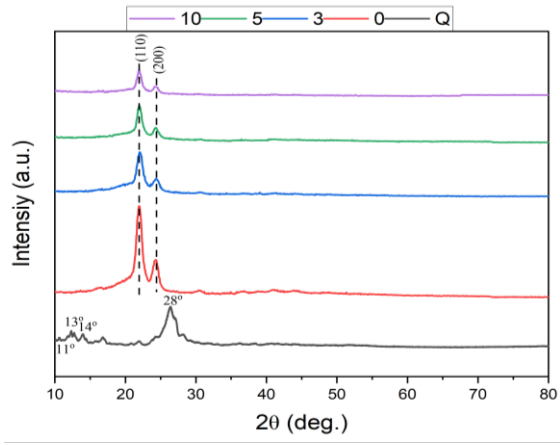

Figure 7. X-ray diffraction (XRD) patterns of pure quercetin (Q), pure PCL mat, and quercetin-loaded polycaprolactone (PCL) electrospun mats with 3, 5, and 10 wt.% quercetin
Note: The prominent peaks for PCL were seen at about 22° and 24°, which corresponded to the (110) and (200) crystalline planes, respectively. Pure quercetin showed its distinctive crystalline peaks at about 11°, 13°, 14°, and 28°.

3.6 Fourier transform infrared spectroscopy

Figure 8 represents the FTIR spectra of PCL mats. The FTIR spectrum was recorded by loading different concentrations of quercetin onto PCL nanofibers to determine the presence of functional groups and confirm the drug entrapment, as summarized in Table 4. The spectrum of the PCL mat was observed to exhibit typical peaks of PCL at 2927 cm^{-1} (asymmetric CH_2 stretching) and 2865 cm^{-1} (symmetric CH_2 stretching) along with a prominent ester carbonyl peak at around 1722 cm^{-1} (C=O stretching) [28]. The spectrum of pure quercetin showed a wide band around 3400 cm^{-1} due to O–H bonding of the phenolic group of quercetin, a prominent aromatic C=O stretching of quercetin at around 1654 cm^{-1} along with C=C stretching of the aromatic ring at approximately 1599 and 1514 cm^{-1} [29].

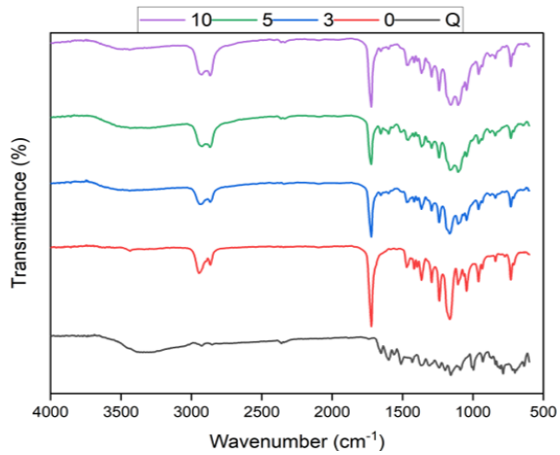

Figure 8. FTIR spectra of pure quercetin, pure PCL mat, and quercetin-loaded PCL electrospun mats
Note: Fourier transform infrared spectroscopy (FTIR), polycaprolactone (PCL).

Table 4. Comparison of FTIR analysis of the characteristic absorption bands of pure quercetin, blank PCL mat, and quercetin-loaded PCL electrospun mats

FTIR Region	Change after Quercetin Loading	Scientific Interpretation
O–H stretching, ~3400 cm^{-1}	Broadening / slight shift	Possible hydrogen bonding or intermolecular interaction
Aromatic carbonyl C=O, ~1654 cm^{-1}	Slight shift/intensity change	Possible interaction between quercetin and the PCL matrix
Phenolic C–O stretching, ~1240 cm^{-1}	Slight shift	Change in the molecular environment of quercetin after incorporation
PCL bands, 2927, 2865, and 1722 cm^{-1}	Retained	Preservation of the PCL backbone without clear chemical degradation

Note: Fourier transform infrared spectroscopy (FTIR), polycaprolactone (PCL).

The FTIR spectrum of pure PCL and PCL-quercetin electrospun mats at a concentration of 3%, 5%, and 10% showed typical absorption of PCL at around 2919 cm^{-1} (CH_2 stretching) along with a prominent ester carbonyl peak at about 1720 cm^{-1}. These bands did not change position with the addition of quercetin, and this suggests there is no alteration in the PCL chemical structure. This reduced transmittance of quercetin-related peaks in the 3600–3200 cm^{-1} and 1650–1600 cm^{-1} ranges shows that there was enhanced absorption due to high drug concentration [18]. According to FTIR results for PCL/Q (quercetin) electrospun fibers, they were similar to the pure PCL, which indicates that the surface chemistry did not change significantly due to quercetin incorporation or the electrospinning process [30].

3.7 Differential scanning calorimetry analysis

The DSC thermograms of pure quercetin and quercetin-loaded PCL nanofiber mats are shown in Figure 9. The DSC thermogram of the pure quercetin exhibited a sharp endothermic peak around 320 °C, which represents the crystal melting transition, followed by an exothermic peak around 388 °C, which could be attributed to the thermal degradation process. The DSC thermogram of PCL mat loaded with quercetin mostly exhibited a melting endothermic peak of PCL at about 64 °C. However, no clear endothermic peak for the melting of quercetin was observed in the composite, implying that quercetin was incorporated in molecular form or had a lower crystallinity/amorphous state in the PCL fiber matrix. This absence of a clear endothermic peak could also be due to the lower drug loading and overlap/sensitivity limitations of DSC towards small crystallites [31]. This finding correlates with the XRD results and may suggest that quercetin was dispersed within the PCL matrix in a less crystalline or amorphous-like state.

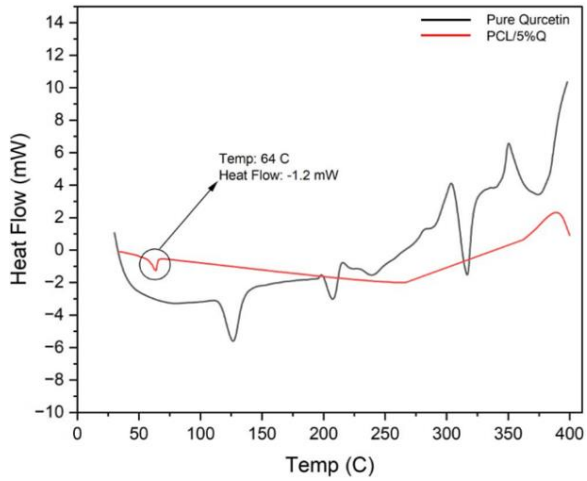

Figure 9. Differential scanning calorimetry (DSC) thermograms for quercetin and polycaprolactone (PCL)/5% quercetin electrospun mats

Nevertheless, the lack of a clear melting peak for quercetin does not constitute a reliable criterion to prove the amorphization of the drug, because its presence can be affected by several factors, such as low quercetin content, overlapping or broad peaks, and the sensitivity of the thermal analysis. From the results of XRD and DSC analyses, it was concluded that quercetin was less crystalline and dispersed well in electrospun fibers; however, additional quantitative crystallinity studies are necessary to determine the precise crystalline nature of quercetin [32, 33].

3.8 Calibration curve of quercetin

The calibration curve of quercetin in the phosphate buffer solution with 0.8% Tween 80 and ethanol with 5% v/v glacial acetic acid is illustrated in Figure 10.

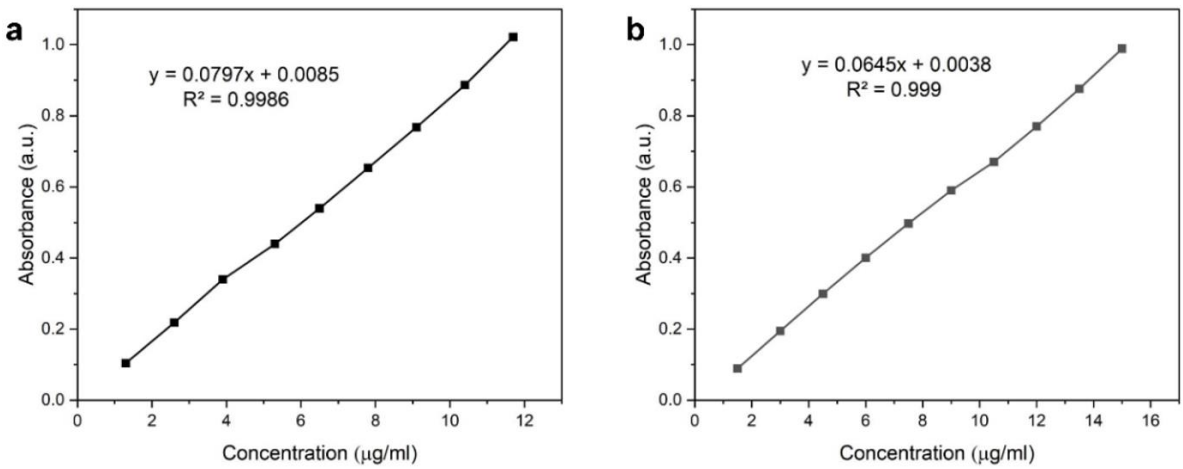

Figure 10. Calibration curves of quercetin in (a) phosphate buffer solution (pH 7.4) and (b) in ethanol

3.9 Saturated solubility

This result indicated that sink conditions were maintained throughout the release study. The solubility study was an essential parameter in characterizing formulations of drugs with poor water solubility. The saturated solubility was 200 µg/ml.

3.10 Encapsulation efficiency

When the drug shows good compatibility with the polymer, has low volatility, and is incorporated at an appropriate concentration, high encapsulation efficiency can be achieved in electrospun nanofiber mats. A further increase in the drug concentration results in a gradual reduction of encapsulation efficiency, likely because the excess drug may form aggregates on the nanofiber surface rather than being encapsulated into the nanofibers. The obtained nanofibers exhibited highly effective entrapment, as presented in Figure 11. Based on the statistical findings, the results indicated that quercetin loading concentration had a significant impact on EE% of the electrospun PCL/Q nanofibers ($p < 0.05$). This means that the effectiveness of the PCL matrix in retaining quercetin was based on the concentration of quercetin.

The differences in EE% can be explained by polymer–drug interactions and electrospinning-related issues. One key factor is the limited drug-loading capacity of the PCL matrix. At higher loading levels, the polymer matrix approaches its saturation limit, beyond which excess quercetin can no longer be effectively encapsulated and is partially excluded from the electrospun fibers as aggregates. A low to moderate quercetin content (1–5%) ensures a good balance between high encapsulation efficiency and stable electrospinning processes. These results highlight the significance of optimal drug concentration for efficient drug incorporation with reproducible nanofiber morphology in wound healing and drug delivery [34].

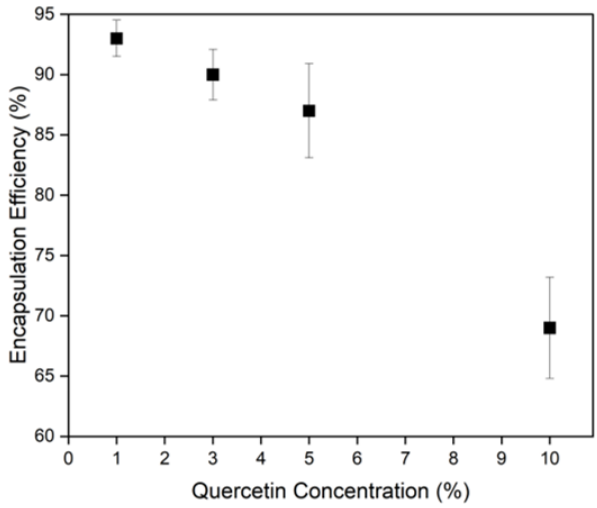

Figure 11. Encapsulation efficiency of polycaprolactone (PCL) mats containing quercetin at varying concentrations
Note: Values were expressed as mean ± SD (n = 3). The statistical analysis was done using one-way ANOVA, where a p-value < 0.05 is significant.

3.11 In vivo wound healing profile

The in vitro release profile of quercetin from the electrospun PCL mats was analyzed using different kinetic models, including zero-order (Eq. (2)), first-order (Eq. (3)), Higuchi (Eq. (4)), and Korsmeyer–Peppas (Eq. (5)). In these models, the cumulative amount of quercetin released was expressed as a function of time, with each model described by its corresponding release rate constant [12]. As shown in Table 5, the release kinetics follow two phases: a burst release phase initially followed by a gradually sustained release phase until the plateau phase [15].

Table 5. Kinetic model fitting parameters of quercetin release from electrospun nanofibrous

Quercetin, wt.%	Zero R^2	First R^2	Higuchi R^2	Korsmeyer n (≤ 60%)	Korsmeyer R^2 (≤ 60%)
1	0.8917	0.9773	0.9827	0.471	0.9760
5	0.8070	0.9395	0.9499	0.494	0.9830
10	0.7251	0.8099	0.9049	0.474	0.9775

$$Q = K_0 \times t \quad (2)$$

$$\ln(Q_0 - Q_t) = lnQ_0 - K_1\, t \quad (3)$$

$$Q = K_H \times t^{0.5} \quad (4)$$

$$Q = K_R \times t^n \quad (5)$$

where, Q is drug fraction, k is kinetic constant, and t is released time.

The initial release was ascribed to the rapid dissolution of quercetin molecules present on or near electrospun PCL fibers in contact with the release medium. This behavior could be attributed to the large surface-to-volume ratio of electrospun fibers. The release rate was observed to gradually decrease as a result of diffusion-controlled drug release in a PCL matrix as a post-rapid dissolution stage. In this stage, restricted diffusion of water in a hydrophobic matrix of electrospun PCL fibers, as well as compaction of electrospun fibers, resulted in sustained release.

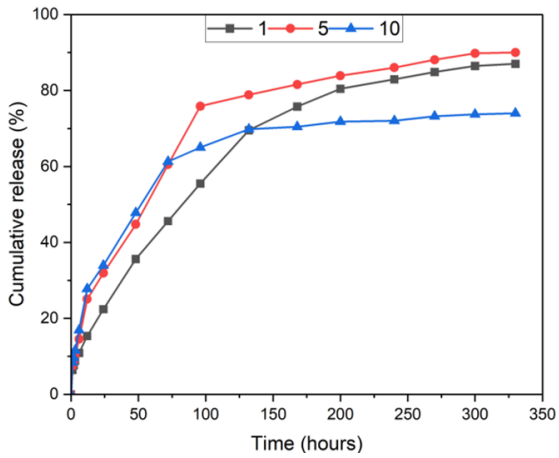

Figure 12. Illustration of the quercetin release profile from polycaprolactone (PCL) electrospun mats (n = 3, independently prepared formulations)

The drug release rate is significantly influenced by the physicochemical properties of PCL. PCL, being hydrophobic and semi-crystalline in nature, does not allow water uptake and movement of drug molecules within PCL, leading to poor drug diffusion in PCL. Quercetin has both hydrophilic and hydrophobic groups present in the molecule, resulting in low miscibility and inhomogeneous distribution of quercetin along with its presence on the surface and then inside PCL. This distribution may explain the initial burst release followed by sustained drug release. Kinetic analysis indicated the best fit of the Higuchi model to the experimental release data for all formulations, suggesting that quercetin release from the electrospun PCL mats was largely driven by diffusion-controlled mechanisms [32]. Importantly, analysis of the Korsmeyer–Peppas model in the early stage of the release process ($M_t/M_\infty \leq 0.6$) demonstrated the diffusion exponent (n) to be below 0.5, thus supporting the Fickian diffusion-controlled release process. This presented an indication that the drug was released from the matrix via molecular diffusion as opposed to the relaxation/erosion process of the polymers [35]. The diffusion-controlled sustained release behavior observed in this study is particularly advantageous for wound-healing applications, as it ensures continuous availability of quercetin during the inflammatory and early proliferative phases, which are critical for effective postoperative wound management. A similar pattern of drug release has also been noted in the case of electrospun poly(ε-caprolactone) (PCL) containing quercetin, wherein drug release was primarily dependent on the hydrophobic nature of the polymer, fiber morphology, and drug distribution and diffusion [36], as schematically illustrated in Figure 12.

3.12 Histological findings

Electrospun PCL mats loaded with quercetin demonstrated satisfactory physicochemical and biological properties, such as adequate mechanical behavior, appropriate degradation rate, and controlled quercetin release, which made them promising materials for use as local drug delivery wound dressings. From among all fabricated specimens, the one composed of 5% quercetin-loaded PCL was chosen for the in vivo investigation due to its superior performance in terms of fiber morphology, encapsulation efficiency, release pattern, and wettability. H&E-stained histological images of the control group without any treatment, blank PCL, and quercetin-loaded PCL wounds after 7, 14, and 21 days post-surgery are shown in Figure 13. Histological analysis aimed to evaluate the degree of tissue regeneration, inflammatory cell infiltration, collagen formation, and re-epithelialization, which are considered essential processes in wound healing.

Figures 13(a), (d), and (g) show the distinguishing characteristics between the experimental groups on day 7 following surgery. The control group without treatment displayed a poor state of tissue repair, characterized by a high degree of inflammation and incomplete epithelialization. The blank PCL group displayed signs of partial recovery, indicating that the PCL material was able to give some support to tissue repair. On the other hand, the PCL mat loaded with quercetin displayed an improved state of tissue repair, with decreased inflammation and initial stages of tissue regeneration. In the control groups: a severely ulcerated surface with a loss of the epidermis and a granular surface with a substance consisting of eosinophilic necrotic debris, fibrin exudates, and chronically infiltrated acute inflammation, indicating the persistence of the inflammation phase and a strong inhibition in the initial healing phase.

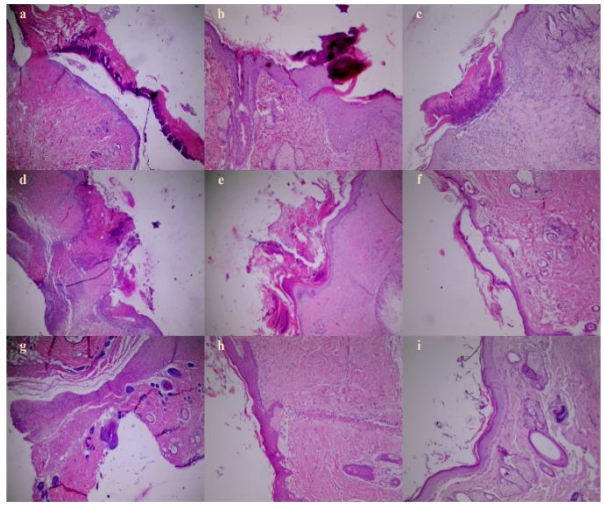

Figure 13. Representative hematoxylin and eosin (H&E)-stained histological samples of wound healing at various stages for the control, pure polycaprolactone (PCL) mat, and PCL mats loaded with quercetin on days 7, 14, and 21 post-surgery: (a-c) represent control samples, (d-f) are pure PCL mat samples, and (g-i) are quercetin-loaded PCL mat samples

On the other hand, in those samples with injuries healed with mats that only had PCL, there was an irregular ulcerated surface with epithelialization associated with necrotic debris and fibrin accumulation. In addition, abundant acute inflammation was seen, showing that it would not play an adequate role in inducing the stimulus of inflammation to decrease inflammation during the healing phases.

However, in the case of wounded tissues treated with the quercetin-loaded PCL mats, the histological features were much improved. There was some re-epithelialization along with the migration of the epithelial cells from the margin of the wounded area. Also, there was marked fibroblast proliferation along with minimal necrosis and inflammation cell infiltration. All these factors indicate the early resolution of the inflammation phase and the onset of the proliferative phase, which is due to the biological activity of quercetin [13, 37].

After 14 days, differences in wound healing among the experimental groups became more evident, as shown in Figures 13(b), (e), and (h). In the untreated control group, wound repair remained delayed, with the presence of slough and necrotic tissue covering the wound surface. The underlying tissue showed an irregular structure with persistent inflammatory cell infiltration and limited evidence of epithelial regeneration.

In the PCL-only mats, although there was moderate healing compared with the control group, the healing process was incomplete. Besides, the area was still below the debris or eschar layer, and the dermis part showed serious penetration of inflammation with an atypical histological structure of the layers in the dermis. All the above aspects indicated that the wound was still in the late proliferative phase with a delay in maturation of the epithelium, along with disorganization of the collagen layer. Conversely, the wounds treated with the quercetin-loaded PCL mats presented a high degree of healing. Histologically, there was a restored and healthy epithelium, and in the dermis, regularly disposed collagen fibers were

observed. Inflammation was minimal to resolving, and there was a good jump towards the remodeling phase, with minimal signs of inflammation. On day 21, as shown in Figures 13(c), (f), and (i), the untreated control group still exhibited poor wound healing, characterized by residual necrotic areas, persistent chronic inflammatory cell infiltration, and incomplete re-epithelialization. The surface of the area of injury showed large areas of poorly healed surfaces that were not in the remodeling phase.

The PCL-only group showed a degree of partial repair. While there was re-epithelialization, it was found that the newly formed epithelium was thin and fragile. Furthermore, there was a noticeable defect in the distance between the newly formed epithelium and the dermis. However, the junction between the epidermis and dermis was also weak. Nevertheless, fibroplasia, rich in immature collagen, was present. This can be considered as a slow rate of maturation of the epithelium [7, 38].

On the other hand, wounds treated with quercetin-loaded PCL mats showed optimal healing. The histological study showed the complete closure of the epithelial layers without any gaps. The dermal side showed strong and heavily matured collagen fibers evenly placed, which indicated an extremely mature stage. There was minimal evidence of inflammation, which ensured complete healing with the completion of the final phase of the inflammatory stage [39, 40]. Overall, the histopathological analysis indicated that the use of quercetin-loaded PCL mats resulted in a significant acceleration of healing compared to the other groups. This is because the inclusion of quercetin resulted in a significant improvement in re-epithelialization, inflammation reduction, and collagenization [41, 42]. On the other hand, the control group displayed delayed wound healing accompanied by persistent signs of inflammation and poor tissue regeneration. Treatment with the blank PCL mats resulted in slight improvement, implying that the scaffold material was capable of providing some assistance in wound healing. Thus, the enhanced healing response seen in the quercetin-loaded PCL group was mostly due to the biological activity of quercetin.

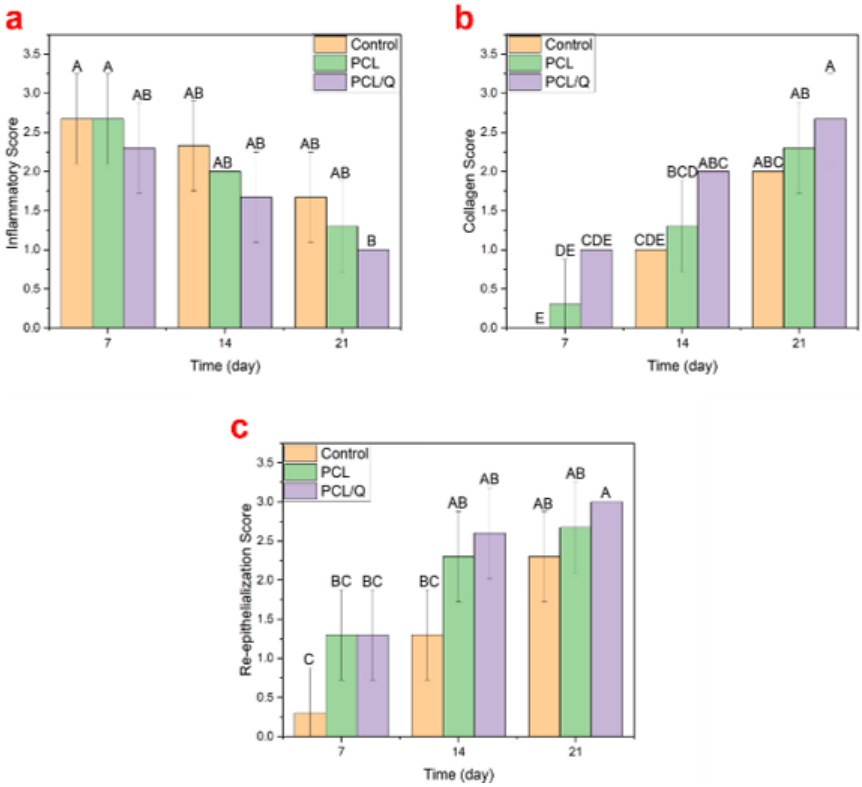

Figure 14. Wound healing histological semi-quantitative assessment of control, polycaprolactone (PCL), and quercetin-loaded PCL-treated samples after 7, 14, and 21 days of surgery: (a) inflammatory score, (b) collagen deposition score, and (c) re-epithelialization score

Note: Values are presented as mean ± SD (n = 3). Analysis of data was carried out by two-way ANOVA followed by Tukey's post hoc test. Different capital letters show significant differences among groups at the same time period ($p < 0.05$).

These results were confirmed by the semi-quantitative evaluation scores presented in Figure 14. The PCL/Q group demonstrated lower levels of inflammation along with better collagen formation and re-epithelialization than those of the control and blank PCL groups ($p < 0.05$). These results suggest that quercetin loading into PCL mats was effective in facilitating wound healing.

4. CONCLUSIONS

The findings of this study suggest that quercetin-loaded electrospun PCL mats may represent a potential approach for the development of post-surgical wound dressings. To facilitate localized and sustained delivery of quercetin, quercetin was incorporated into PCL nanofibers to facilitate localized and sustained drug delivery. The fabricated mats showed a continuous fibrous structure, efficient drug entrapment, and retention of quercetin mainly in an amorphous state, without clear indication for degradation of the drug. Furthermore, the in vivo results indicated that quercetin-infused PCL mats exhibited enhanced histological parameters of wound healing compared with the control and unloaded PCL groups. This improvement might be due to the presence

of improved tissue organization, increased collagen deposition, reduced inflammatory response, and enhanced epithelialization by day 21. The beneficial impact of quercetin may be related to its anti-inflammatory and antioxidant effects that can aid in tissue regeneration. Nonetheless, further experiments are recommended to confirm the efficacy of the proposed materials in surgical wound applications.

ACKNOWLEDGMENT

The authors would like to thank the College of Pharmacy, Mustansiriyah University, for technical support.

REFERENCES

[1] Mahyudin, F., Edward, M., Basuki, M.H., Basrewan, Y., Rahman, A. (2020). Modern and classic wound dressing comparison in wound healing, comfort and cost. Jurnal Ners, 15(1): 31-36. https://doi.org/10.20473/jn.v15i1.16597

[2] Mirhaj, M., Labbaf, S., Tavakoli, M., Seifalian, A.M. (2022). Emerging treatment strategies in wound care. International Wound Journal, 19(7): 1934-1954. https://doi.org/https://doi.org/10.1111/iwj.13786

[3] Holmes, S.P., Rivera, S., Hooper, P.B., Slaven, J.E., Que, S.K.T. (2022). Hydrocolloid dressing versus conventional wound care after dermatologic surgery. JAAD International, 6: 37-42. https://doi.org/10.1016/j.jdin.2021.11.002

[4] Nur, M.G., Rahman, M., Dip, T.M., Hossain, M.H., et al. (2025). Recent advances in bioactive wound dressings. Wound Repair and Regeneration, 33(1): e13233. https://doi.org/https://doi.org/10.1111/wrr.13233

[5] Yu, D.G., He, W., He, C., Liu, H., Yang, H. (2025). Versatility of electrospun Janus wound dressings. Nanomedicine, 20(3): 271-278. https://doi.org/10.1080/17435889.2024.2446139

[6] Oleiwi, A.H., Dal fi, H.K. (2025). A comprehensive review on electrospinning: Mechanisms, functional modifications and the importance of nanofiber systems. International Journal of Nanoscience, 24(6): 2530002. https://doi.org/10.1142/S0219581X25300020

[7] Fahimirad, S., Abtahi, H., Satei, P., Ghaznavi-Rad, E., Moslehi, M., Ganji, A. (2021). Wound healing performance of PCL/chitosan based electrospun nanofiber electrosprayed with curcumin loaded chitosan nanoparticles. Carbohydrate Polymers, 259: 117640. https://doi.org/10.1016/j.carbpol.2021.117640

[8] Obead, N.K., Arif, I.S., Waheed, H.J., Batiha, G.E.S. (2025). Quercetin improves the histopathological changes of liver caused by interferon beta 1b-induced liver injury. Al Mustansiriyah Journal of Pharmaceutical Sciences, 25(2): 258-265. https://doi.org/10.32947/ajps.v25i2.1153

[9] Hameed, G.S., Hanna, D.B., Naama, N. (2025). Solubility enhancement of cefdinir using different pharmaceutical approaches for enhancement of the drug performance. Iraqi Journal of Pharmaceutical Sciences, 34(1): 122-132. https://doi.org/10.31351/vol34iss1pp122-132

[10] Oleiwi, A.H., Jabur, A.R., Alsalhy, Q.F. (2023). Morphology of polystyrene nano-fiber membranes reinforced with copper oxide and zirconium oxide nanoparticles as a sulfur absorbent materials. AIP Conference Proceedings, 2769(1): 020065. https://doi.org/10.1063/5.0129144

[11] Alsaide, N.H., Maraie, N.K. (2023). Insights into medicated films as attractive dosage forms. Al Mustansiriyah Journal of Pharmaceutical Sciences, 23(1): 1-13. https://doi.org/10.32947/ajps.v23i1.981

[12] Viscusi, G., Paolella, G., Lamberti, E., Caputo, I., Gorrasi, G. (2023). Quercetin-loaded polycaprolactone-polyvinylpyrrolidone electrospun membranes for health application: Design, characterization, modeling and cytotoxicity studies. Membranes, 13(2): 242. https://doi.org/10.3390/membranes13020242

[13] Faraji, S., Nowroozi, N., Nouralishahi, A., Shayeh, J.S. (2020). Electrospun poly-caprolactone/graphene oxide/quercetin nanofibrous scaffold for wound dressing: Evaluation of biological and structural properties. Life Sciences, 257: 118062. https://doi.org/10.1016/j.lfs.2020.118062

[14] Rohatgi, N., Ganapathy, D., Sathishkumar, P. (2023). Eradication of Pseudomonas aeruginosa biofilm using quercetin-mediated copper oxide nanoparticles incorporated in the electrospun polycaprolactone nanofibrous scaffold. Microbial Pathogenesis, 185: 106453. https://doi.org/10.1016/j.micpath.2023.106453

[15] Karuppannan, S.K., Dowlath, M.J.H., Ramalingam, R., Musthafa, S.A., et al. (2022). Quercetin functionalized hybrid electrospun nanofibers for wound dressing application. Materials Science and Engineering: B, 285: 115933. https://doi.org/10.1016/j.mseb.2022.115933

[16] Fernández, J., Ruiz-Ruiz, M., Sarasua, J.R. (2019). Electrospun fibers of polyester, with both nano-and micron diameters, loaded with antioxidant for application as wound dressing or tissue engineered scaffolds. ACS Applied Polymer Materials, 1(5): 1096-1106. https://doi.org/10.1021/acsapm.9b00108

[17] Lu, B., Huang, Y., Chen, Z., Ye, J., Xu, H., Chen, W., Long, X. (2019). Niosomal nanocarriers for enhanced skin delivery of quercetin with functions of anti-tyrosinase and antioxidant. Molecules, 24(12): 2322. https://doi.org/10.3390/molecules24122322

[18] Hu, Y., Fu, Z., Yang, S., Zhou, Y., et al. (2024). A multifunctional quercetin/polycaprolactone electrospun fibrous membrane for periodontal bone regeneration. Materials Today Bio, 24: 100906. https://doi.org/10.1016/j.mtbio.2023.100906

[19] Medeiros, G.B., Lima, F.D.A., de Almeida, D.S., Guerra, V.G., Aguiar, M.L. (2022). Modification and functionalization of fibers formed by electrospinning: A review. Membranes, 12(9): 861. https://doi.org/10.3390/membranes12090861

[20] Mukasheva, F., Adilova, L., Dyussenbinov, A., Yernaimanova, B., Abilev, M., Akilbekova, D. (2024). Optimizing scaffold pore size for tissue engineering: Insights across various tissue types. Frontiers in Bioengineering and Biotechnology, 12: 1444986. https://doi.org/10.3389/fbioe.2024.1444986

[21] Ortiz-Marqués, A., Caldevilla, P., Goldmann, E., Safuta, M., Fernández-Raga, M., Górski, M. (2025). Porosity and permeability in construction materials as key parameters for their durability and performance: A review. Buildings, 15(18): 3422. https://doi.org/10.3390/buildings15183422

[22] Hammadi, A.F., Oleiwi, A.H., Abdalameer, T.A., Al-Obaidi, A.J. (2023). Effect of alumina particles on the mechanical and physical properties of polypropylene whisker reinforced lamination 80: 20 resin composite. Revue des Composites et des Matériaux Avancés-Journal of Composite and Advanced Materials, 33(1): 7-12. https://doi.org/10.18280/rcma.330102

[23] Wiegand, C., Wesenberg, U., Heggemann, J. (2023). A moisture-balancing hydropolymer gel dressing with a tissue boost effect-experimental and clinical evidence. Chronic Wound Care Management and Research, 10: 11-21. https://doi.org/10.2147/CWCMR.S42249

[24] Feng, Y., Jupei, Z., Dong, Z., Tang, L. (2023). Characterization, biocompatibility, and optimization of electrospun SF/PCL composite nanofiber films. Reviews on Advanced Materials Science, 62(1): 20220333. https://doi.org/10.1515/rams-2022-0333

[25] García-Casas, I., Montes, A., Valor, D., Pereyra, C., Martinez de la Ossa, E.J. (2019). Foaming of polycaprolactone and its impregnation with quercetin using supercritical CO_2. Polymers, 11(9): 1390. https://doi.org/10.3390/polym11091390

[26] Sanchez-Rexach, E., Iturri, J., Fernandez, J., Meaurio, E., Toca-Herrera, J.L., Sarasua, J.R. (2019). Novel biodegradable and non-fouling systems for controlled-release based on poly (ε-caprolactone)/Quercetin blends and biomimetic bacterial S-layer coatings. RSC Advances, 9(42): 24154-24163. https://doi.org/10.1039/C9RA04398E

[27] Li, S.F., Hu, T.G., Wu, H. (2024). Development of quercetin-loaded electrospun nanofibers through shellac coating on gelatin: Characterization, colon-targeted delivery, and anticancer activity. International Journal of Biological Macromolecules, 277: 134204. https://doi.org/10.1016/j.ijbiomac.2024.134204

[28] Gedik, B., Erdem, M.A. (2025). Electrospun PCL membranes for localized drug delivery and bone regeneration. BMC Biotechnology, 25(1): 31. https://doi.org/10.1186/s12896-025-00965-7

[29] Wangsawangrung, N., Choipang, C., Chaiarwut, S., Ekabutr, P., et al. (2022). Quercetin/hydroxypropyl-β-cyclodextrin inclusion complex-loaded hydrogels for accelerated wound healing. Gels, 8(9): 573. https://doi.org/10.3390/gels8090573

[30] Oleiwi, A.H., Jabur, A.R., Alsalhy, Q.F. (2021). Polystyrene/Mwcnts nanofiber membranes characterizations in reducing sulfur content in crude oil. Key Engineering Materials, 886: 86-96. https://doi.org/10.4028/www.scientific.net/KEM.886.86

[31] Ayran, M., Dirican, A.Y., Saatcioglu, E., Ulag, S., et al. (2022). 3D-printed PCL scaffolds combined with juglone for skin tissue engineering. Bioengineering, 9(9): 427. https://doi.org/10.3390/bioengineering9090427

[32] Ayran, M., Karabulut, H., Deniz, K.I., Akcanli, G.C., et al. (2023). Electrically triggered quercetin release from polycaprolactone/bismuth ferrite microfibrous scaffold for skeletal muscle tissue. Pharmaceutics, 15(3): 920. https://doi.org/10.3390/pharmaceutics15030920

[33] Fo'ad, T., Hameed, G.S., Raauf, A.M. (2022). Thermal analysis in the pre-formulation of amorphous solid dispersion for poorly water-soluble drugs. International Journal of Drug Delivery Technology, 12: 1595-1599. https://doi.org/10.25258/ijddt.12.4.19

[34] Böncü, T.E., Ozdemir, N. (2022). Effects of drug concentration and PLGA addition on the properties of electrospun ampicillin trihydrate-loaded PLA nanofibers. Beilstein Journal of Nanotechnology, 13(1): 245-254. https://doi.org/10.3762/bjnano.13.19

[35] Huo, P., Han, X., Zhang, W., Zhang, J., Kumar, P., Liu, B. (2021). Electrospun nanofibers of polycaprolactone/collagen as a sustained-release drug delivery system for artemisinin. Pharmaceutics, 13(8): 1228. https://doi.org/10.3390/pharmaceutics13081228

[36] Korsmeyer, R.W., Gurny, R., Doelker, E., Buri, P., Peppas, N.A. (1983). Mechanisms of solute release from porous hydrophilic polymers. International Journal of Pharmaceutics, 15(1): 25-35. https://doi.org/10.1016/0378-5173(83)90064-9

[37] Huang, H.C., Chen, Y., Hu, J., Guo, X.T., et al. (2024). Quercetin and its derivatives for wound healing in rats/mice: Evidence from animal studies and insight into molecular mechanisms. International Wound Journal, 21(2): e14389. https://doi.org/https://doi.org/10.1111/iwj.14389

[38] Du, M., Liu, S., Lan, N., Liang, R., et al. (2024). Electrospun PCL/gelatin/arbutin nanofiber membranes as potent reactive oxygen species scavengers to accelerate cutaneous wound healing. Regenerative Biomaterials, 11: rbad114. https://doi.org/10.1093/rb/rbad114

[39] Voiță-Mekereș, F. (2024). Assessment of the embryological origin, anatomical and histological structure of the skin. Archives of Pharmacy Practice, 15(2-2024): 69-74. https://doi.org/10.51847/SWViK4kyKx

[40] Masson-Meyers, D.S., Andrade, T.A., Caetano, G.F., Guimaraes, F.R., Leite, M.N., Leite, S.N., Frade, M.A.C. (2020). Experimental models and methods for cutaneous wound healing assessment. International Journal of Experimental Pathology, 101(1-2): 21-37. https://doi.org/10.1111/iep.12346

[41] Mi, Y., Zhong, L., Lu, S., Hu, P., et al. (2022). Quercetin promotes cutaneous wound healing in mice through Wnt/β-catenin signaling pathway. Journal of Ethnopharmacology, 290: 115066. https://doi.org/10.1016/j.jep.2022.115066

[42] Gomathi, K., Gopinath, D., Ahmed, M.R., Jayakumar, R. (2003). Quercetin incorporated collagen matrices for dermal wound healing processes in rat. Biomaterials, 24(16): 2767-2772. https://doi.org/10.1016/S0142-9612(03)00059-0